Int J Clin Exp Med 2022;15(11):368-385
www.ijcem.com /ISSN:1940-5901/IJCEM0145535

Original Article

Exploring the pharmacodynamic material basis of the nootropic effect of Cynomorium ethyl acetate based on serum medicinal chemistry and network pharmacology

Da Wang[1], Han Luo[3], Shuhui Wang[2], Zhibin Xiao[1], Ruilan Han[1]

Departments [1]School of Pharmacy, [2]School of Nursing, Inner Mongolia Medical University, Hohhot 010110, Inner Mongolia Autonomous Region, China; [3]Inner Mongolia Medical Device Inspection Institute, Hohhot 010020, Inner Mongolia Autonomous Region, China

Received July 25, 2022; Accepted September 14, 2022; Epub November 15, 2022; Published November 30, 2022

Abstract: Objective: Analyzing Cynomorium ethyl acetate extract and medicated serum components, while combining results with network pharmacology to explore the possible pharmacodynamic material basis of its nootropic effect. Methods: Preparation of Cynomorium ethyl acetate extract, Cynomorium ethyl acetate medicated serum in rats and blank serum in rats; HPLC-Q-Exactive-MS/MS technology to qualitative analysis of Cynomorium ethyl acetate extract, medicated serum and blank serum, comparison of the mass spectra of the three, combined with Xcalibur 3.0 software to analyze the transition components and their metabolites in rat blood; combined with network pharmacology to constructed the network diagram of Cynomorium ethyl acetate medicated serum components-disease targets, screened key compounds and key targets, and the targets were analyzed by Gene Ontology (GO) and Kyoto Encyclopedia of Genes and Genomes (KEGG) pathway analysis. Results: A total of 17 substances were detected in Cynomorium ethyl acetate extract, including 3 flavonoids, 3 triterpenoids, 7 organic acids, 2 volatile components, 1 alkaloid and 1 other species; A total of 18 substances were detected in the medicated serum, including 3 prototype components and 15 metabolites of prototype components. We used network pharmacology to obtain 10 core components in the medicated serum, such as 9, 10-dihydroxystearic acid, naringenin methylation, octadecenedioic acid, and oleic acid, etc. Obtained 13 core targets such as steroid receptor coactivator (SRC), mitogen-activated protein kinase 1 (MAPK1), phosphatidylinositol-4, 5-bisphosphate 3-kinase catalytic subunit alpha (PIK3CA), etc. We infer that Cynomorium ethyl acetate may exert nootropic effects through reactive astrocytes (RAS), mitogen-activated protein kinases (MAPK), hypoxia-inducible factor-1 (HIF-1), and calcium signaling pathways. Conclusion: This study analyzed and identified the components of Cynomorium ethyl acetate extract and medicated serum, and the possible pharmacodynamic material basis of the nootropic effect was explored, which provided a reference for clarifying the mechanism of Cynomorium ethyl acetate.

Keywords: Cynomorium ethyl acetate, prototype components, metabolites, pharmacodynamic material basis, network pharmacology

Introduction

Alzheimer's disease (AD), also known as senile dementia, is an age-related irreversible neurodegenerative disease. Around the world, nearly 37 million people are affected by AD, and it is speculated that AD will be the third leading cause of death in the elderly after cancer and heart disease in the next few years [1]. The pathogenesis of AD is extremely complex, with multiple factors interrelated and multiple targets interacting. At present, there is no specific drug for AD treatment. However, as part of the precious heritage of the Chinese nation, traditional Chinese medicine has significant advantages in the treatment of AD with its multi-components and multi-targets.

Cynomorium is a perennial succulent parasitic herb, it is a traditional Chinese medicine commonly utilized in China. It is basically disseminated from inner Mongolia, Xinjiang, Ningxia, Qinghai and other northwestern regions. It has pharmacological effects such as scavenging

free radicals, anti-oxidation, neuroprotective, immunity-improving, aphrodisiac, anti-inflammatory and anti-tumor [2]. Previous research by our research group found that Cynomorium water extract and Cynomorium alcohol extract can improve the learning and memory ability of mice that have undergone an aging model, but the difference is not significant. The ethyl acetate extract of Cynomorium is the best for improving the learning and memory ability of mice that have undergone an aging model. We pointed out that the active site of Cynomorium to improve the learning and memory ability of these mice is the ethyl acetate site. Cynomorium ethyl acetate extract can significantly improve the learning and memory ability of aging modeled mice, as well as increase the ability of these mice to scavenge free radicals and reduces the damage of free radicals to neurons in the CA1 region of the hippocampus of mice. Other researchers have found that Cynomorium ethyl acetate extract can improve cognitive dysfunction in mice and up-regulate the protein expressions of P-Erk1/2 and P-CREB in the MAPK/EK1/2 signaling pathway [3, 4]. However, there is no literature report on the pharmacodynamic material basis of the nootropic effect of Cynomorium ethyl acetate. In this experiment, we used HPLC-Q-Exactive-MS/MS technology to analyze Cynomorium ethyl acetate extract, medicated serum, blank serum, and determined its prototype components and metabolites that migrated into the blood, combined with network pharmacology to predict the target of substances that migrate into the blood, and completed GO and KEGG enrichment pathway analysis, as well as explored the possible pharmacodynamic material basis of its nootropic effect, and provided a reference to further confirm the nootropic mechanism of Cynomorium ethyl acetate in the future.

Materials and methods

Plant material, animals, reagents and chemicals

Cynomorium was purchased from Anguo Jiuwang Pharmaceutical Co., Ltd., Batch number: 20132617, and was identified by Professor Qubi of Inner Mongolia Medical University. Twenty SD rats, body weight (200±20) g, male, purchased from Experimental Animal Center of Inner Mongolia Medical University, SPF grade, laboratory animal production license number/certificate number: SCXK (Mongolia) 2020-0001, Breeding environment: Experimental Animal Center of Inner Mongolia Medical University, humidity (45±5)%, temperature (22±1)°C. Animal experiments were approved by the Medical Ethics Committee of Inner Mongolia Medical University (Document number: YKD-2019019). Chromatographic grade acetonitrile was purchased from Thermo Fisher (USA, Lot: 106246). Chromatographic grade formic acid was purchased from Thermo Fisher (USA, Lot: 110301). Petroleum ether was purchased from Tianjin Jindong Tianzheng Chemical Reagent Co., Ltd. (Lot: 15894-2008). Ethyl acetate was purchased from Tianjin Jindong Tianzheng Chemical Reagent Co., Ltd. (Lot: 12589-2007). Carboxymethylcellulose sodium was purchased from Tianjin Yongda Chemical Reagent Co., Ltd. (Lot: 20140422). Thermo Ulti Mate3000 fast ultra-high performance liquid chromatograph (Thermo Fisher, USA); Q-Exactive liquid chromatography-mass spectrometry system (Thermo Fisher, USA); Supersil C8 column (2.1 mm × 100 mm, 5 μm SN: 20201A802, Dalian Yilite Analytical Instrument Co., Ltd.); KQ-400-DE Ultrasonic apparatus (Kunshan Ultrasonic Instrument Co., Ltd.); MX-S mixer (Dalong Xingchuang Experimental Instrument Co., Ltd.); BSA124S Electronic Analytical Balance (Sartorius Scientific Instruments Co., Ltd.); FW177 Pulverizer (Taisite Instrument Co., Ltd.); 3-18K cryogenic centrifuge (SIGMA, Italy); OSB-2100 Rotary Evaporator (Shanghai Ailang Instrument Co., Ltd.); ForMa900SERIES ultra-low temperature refrigerator (Thermo Fisher, USA).

Analysis of Cynomorium ethyl acetate extract components and medicated serum components

Preparation of Cynomorium ethyl acetate extract: Pulverize Cynomorium with a pulverizer and pass through a 40-mesh sieve, weigh Cynomorium powder 600 g, soak with 1.8 L petroleum ether for 2 hours and filter it, discard the filtrate, wait for the filter residue to dry until there is no petroleum ether smell, then add 3 L of ethyl acetate to soak for 30 min, simmer for 1 hour, filter and take the filtrate, concentrated by rotary evaporator, dried and weighed, 1.82 g of Cynomorium ethyl acetate extract obtained, store Cynomorium ethyl acetate extract at 4 degrees for subsequent experiments.

Preparation of medicated serum: Twenty SD rats were randomly divided into the administration group and the control group, with 10 rats in each group. After 3 days of adaptive feeding, from the 4th day, Cynomorium ethyl acetate extract was dissolved in 0.5% carboxymethylcellulose sodium to make a suspension, administered by gavage at a concentration of 83 mg/kg (Calculated according to the equivalent dose ratio table converted from the body surface area of humans and animals, which is 6.3 times the conventional dose), once a day at the same time for 10 days. At the same time, the control group was given the same dose of normal saline as the administration group. Animals were fasted for 12 hours before the last administration. Then 1.5 hours after the last administration, the rats were anesthetized by intraperitoneal injection of 5% chloral hydrate (6 mL/kg), and we opened the abdominal cavity, where blood was collected from the abdominal aorta, centrifuged the blood in a cryogenic centrifuge at 3500 $r \cdot min^{-1}$ for 5 min; we then aspirated the pale yellow transparent liquid in the upper layer of the centrifuge tube, subpackaged it and it was frozen in the freezer at -80 degrees for later use.

Treatment of medicated serum: A total of 100 μL of the medicated serum was taken out from the freezer at -80 degrees, placed in the refrigerator at 4 degrees to thaw, and 300 μL of acetonitrile was added after thawing and quickly mixed with a mixer for protein precipitation. The suspension was placed in a cryogenic centrifuge at 4 degrees, 16000 $r \cdot min^{-1}$, centrifuged for 10 min, and the supernatant was taken for analysis.

Chromatographic conditions: Chromatographic column: Supersil C8 (2.1 mm × 100 mm, 5 μm). The mobile phase was acetonitrile (A)-0.1% formic acid water (C). The gradient elution program was: 0-5 min, 30%-30% (A); 5-20 min, 30%-90% (A); 20-50 min, 90%-95% (A); 50-50.1 min, 95%-30% (A); 50.1-60 min, 30%-30% (A), flow rate of 0.2 mL/min, the sample was automatically injected at 4 degrees, injection volume of 5 μL, column temperature of 40 degrees.

MS spectrometer conditions: Electrospray ionization (ESI) was used for positive/negative ion detection, and mass spectral information was acquired in full-scan mode. The mass spectrometry conditions are as follows: 1. Sheath gas flow rate: 40 L/min; 2. Aux gas flow rate: 2 L/min; 3. Spray voltage: 3.5 KV; 4. Capillary temperature: 350°C; 5. S-lens RF level: 50 KV; 6. Aux gas heater temperature: 150°C.

Network pharmacology research

Collection the targets of Cynomorium ethyl acetate medicated serum components: In this study, we obtained the components of Cynomorium ethyl acetate medicated serum from HPLC-Q-Exactive-MS/MS analysis, the SwissTargetPrediction (http://www.swisstargetprediction.ch/) and Superpred (https://prediction.charite.de/) websites were used to input compound structures and predict compound targets. Then, the compound component targets obtained from the two databases were summarized and deduplicated, and were used as the targets of Cynomorium ethyl acetate medicated serum components.

Collection the targets of AD: In this study, the main disease targets of AD were obtained in the TTD (http://db.idrblab.net/ttd/) database, OMIM (https://www.omim.org/) database, GeneCards (https://www.uniprot.org/) database and DrugBank (https://go.drugbank.com/) database respectively, using "Alzheimer's disease" as the search term.

Cynomorium ethyl acetate medicated serum components-AD disease network construction: Intersection of the data obtained in 2.3.1 and 2.3.2, the Venn diagram was drawn by Venny (https://bioinfogp.cnb.csic.es/tools/venny/), and the common targets of Cynomorium ethyl acetate medicated serum components-AD disease were obtained. We used STRING (https://cn.string-db.org/) platform and Cytoscape 3.9.0 software to construct a component-target network diagram. The nodes represent the targets of Cynomorium ethyl acetate medicated serum components and the potential target genes. The edges represent the relationship between Cynomorium ethyl acetate medicated serum components and its targets. Therefore, the connection situation can screen out the key compounds of Cynomorium ethyl acetate medicated serum components that act on AD diseases.

Protein-protein interaction (PPI) network construction: We imported the common targets

of Cynomorium ethyl acetate medicated serum components-AD disease into the STRING (https//cn.string-db.org/) database for PPI analysis, the Organism was selected as "Homo sapiens". The obtained results were imported into Cytoscape 3.9.0 software in the form of text for visual analysis; nodes whose Degree, Betweenness, and Closeness are all greater than the average were selected as key targets.

Gene ontology (GO) and kyoto encyclopedia of genes and genomes (KEGG) enrichment analysis: The DAVID (http://david.ncifcrf.gov/) database was used to perform GO and KEGG enrichment analysis on the intersection targets obtained from Cynomorium ethyl acetate medicated serum components-AD disease. Taking $P<0.05$ as the threshold, they were sorted in ascending order of *P* value, and the significantly enriched entries or pathways were screened. Among them, the GO enrichment analysis included biological process (BP), cellular component (CC) and molecular function (MF).

Results

Analysis of components of Cynomorium ethyl acetate extract

Total ion chromatogram is a plot of the sum of all ion intensities over time or number of scans in a selected mass range. HPLC-Q-Exactive-MS/MS technology was used to qualitatively analyze the components of Cynomorium ethyl acetate extract, and total ion chromatogram in positive and negative ion modes were obtained, as shown in **Figure 1**. Xcalibur 3.0 software was used to obtain the fragment information of the primary and secondary mass spectrometry of the compounds. Combined with literature reports and according to the cracking rules of different compounds, we compared the theoretical values and measured values, and a total of 17 compounds were identified in the Cynomorium ethyl acetate extract, including: catechin, naringenin, adenosine, salicylic acid, 2 (S)-naringenin-4-O-lic glucopyranoside, ursolic acid, acetyl ursolic acid, ursolic acid hydrogen malonate, capilliplactone, gallic acid, protocatechuate, vanillic acid, p-hydroxybenzoic acid, p-hydroxycinnamic acid, oleic acid, palmitic acid, octadecenedioic acid, as shown in **Table 1**.

Analysis of components of Cynomorium ethyl acetate medicated serum

Blank serum samples and medicated serum samples were analyzed by HPLC-Q-Exactive-MS/MS technology, and total ion chromatograms in positive and negative ion modes were obtained, as shown in **Figures 2** and **3**. According to the Cynomorium ethyl acetate extract chemical composition identification method and literature reports, Xcalibur 3.0 software was used to obtain the fragment information of the primary and secondary mass spectrometry of the compounds. Then, we compared the components of Cynomorium ethyl acetate extract, medicated serum, and blank serum samples, and initially detected 18 compounds in medicated serum, including 3 prototype components and 15 metabolites, of which the prototype components are: oleic acid, palmitic acid and octadecenedioic acid. The metabolites are: methylation of naringenin, glucuronidation of protocatechuic acid and glucuronated O-Methy of protocatechuic acid, methylation of vanillic acid, hydrolysis and glucuronidation of vanillic acid, oxidation of oleic acid, acetylation of catechin, sulfate esterification of salicylic acid, hydroxylation and glucuronidation of salicylic acid, deoxidation of salicylic acid, methylation of p-hydroxybenzoic acid, sulfate esterification of p-hydroxybenzoic acid, deoxidation of p-hydroxybenzoic acid, hydroxylation and glucuronidation of p-hydroxybenzoic acid, as shown in **Tables 2** and **3**.

Identification of components of Cynomorium ethyl acetate extract

In this study, a total of 17 components were characterized and identified in Cynomorium ethyl acetate extract, and compound 2, compound 10 and compound 11 were used as examples to illustrate the inferred process.

Compound 2: In the negative ion mode, the quasimolecular ion peak m/z 271 [M+H] -, retention time 14.95 min, and the molecular formula of C15H12O5 was obtained. There are mainly fragment ions at m/z 151 and m/z 107 in the MS spectrum, Among them, m/z 151 has a loss of a phenol group and a carbonyl group by the RDA cleavage of the C ring, and m/z 107 is produced by the cleavage of the A ring and

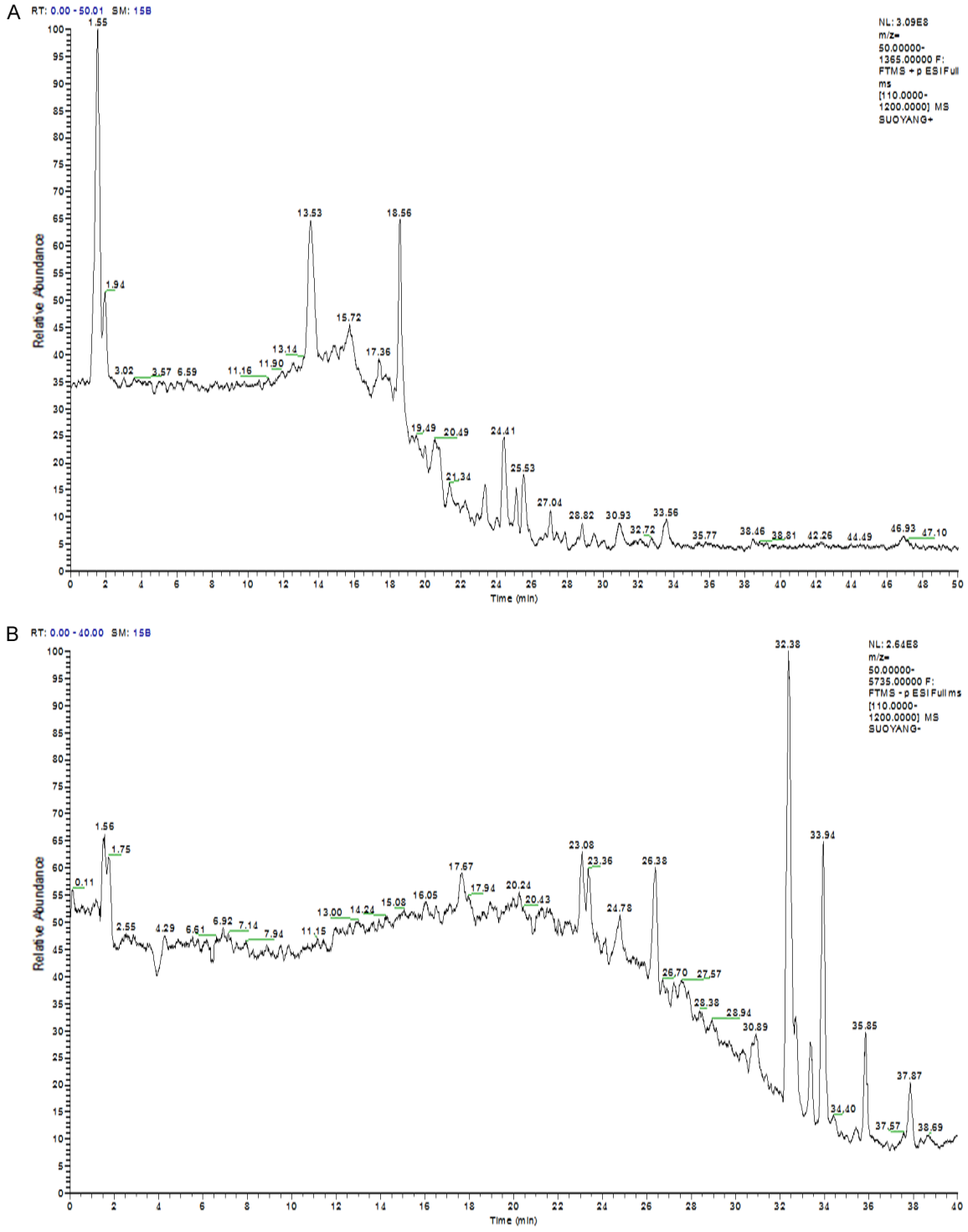

Figure 1. Total ion chromatograms of Cynomorium ethyl acetate extract (a/b indicates positive/negative ions).

the RDA cleavage of the C ring. By comparing with a literature report [5], compound 2 was identified as naringenin, the secondary mass spectrum in negative ion mode is shown in **Figure 4A**.

Compound 10: In the negative ion mode, the quasimolecular ion peak m/z 169 [M+H] -, retention time 1.7 min, and the molecular formula of C7H6O5 was obtained. There are mainly fragment ions of m/z 125 in its secondary

Table 1. The mass spectrometry information of compounds in Cynomorium ethyl acetate extract

NO.	retention time/ min	Ion mode	molecular weight		Mass error (ppm)	MS/MS Fragments	Compound	Molecular formula
			Theoretical value	measured value				
1	1.45	[M+H] +	291.08631	291.08203	-1.47723	191.03, 123.04, 90.98	catechin	C15H1406
2	14.95	[M+H] -	271.0601	271.06238	2.4114	177.02, 151, 107.01	naringenin	C15H1205
3	1.37	[M+H] +	268.10403	268.10339	-2.3871	203.02, 135.06, 84.96	adenosine	C10H1304N5
4	2.68	[M+H] -	137.02332	137.02374	3.0652	119.01, 93.03, 87.92	salicylic acid	C7H603
5	5.82	[M+H] -	433.11292	433.11536	2.6336	289.04, 271.06, 257.09	2 (S)-naringenin-4-O-β-D-glucopyranoside	C21H22010
6	30.7	[M+H] -	455.35197	455.35522	4.1373	279.23, 172.95, 115.92	ursolic acid	C30H4803
7	33.99	[M+H] -	497.36254	497.36569	4.3334	455.36, 427.15, 397.28	acetyl ursolic acid	C32H5004
8	29.83	[M+H] -	541.35237	541.35529	4.3939	497.37, 455.36, 84.99	ursolic acid hydrogen malonate	C33H5006
9	1.73	[M+H] -	131.03389	131.03435	3.5105	113.02, 87.04, 72.99	capilliplactone	C5H804
10	1.7	[M+H] -	169.01315	169.01382	3.9642	152.03, 139.04, 125.02	gallic acid	C7H605
11	1.78	[M+H] -	153.01824	153.01884	3.9211	123.04, 109.03, 96.96	protocatechuic acid	C7H604
12	1.72	[M+H] -	167.03389	167.03461	4.3105	152.03, 123.04, 109.03	vanillic acid	C8H804
13	2.68	[M+H] -	137.02332	137.02382	3.649	119.01, 93.03, 72.97	p-hydroxybenzoic acid	C7H603
14	3.91	[M+H] -	163.03897	163.03961	3.9254	119.05, 93.03, 73.03	p-hydroxycinnamic acid	C9H803
15	34.07	[M+H] -	281.24751	281.24982	4.2134	210.12, 158.41, 124.63	oleic acid	C18H3402
16	33.37	[M+H] -	255.23186	255.23386	3.836	219.85, 158.42, 117.06	palmitic acid	C16H3202
17	23.76	[M+H] -	311.22169	311.22421	4.0971	293.21, 211.13, 171.10	octadecenedioic acid	C18H3204

mass spectrum, which is formed by the loss of CO_2 from the parent ion. By comparing with a literature report [6], its retention time and mass spectrometry data are consistent with gallic acid, so compound 10 was identified as gallic acid, the secondary mass spectrum in negative ion mode is shown in **Figure 4B**.

Compound 11: In the negative ion mode, the quasimolecular ion peak m/z 153 [M+H] -, retention time 1.78 min, and the molecular formula of C7H604 was obtained. There were mainly fragment ions of m/z 109 in its secondary mass spectrum, which is formed by the loss of CO_2 from the parent ion. By comparing with the literature [7], its retention time and mass spectrometry data are consistent with protocatechuic acid, so compound 11 was identified as protocatechuic acid, the secondary mass spectrum in negative ion mode is shown in **Figure 4C**.

Identification of metabolite in medicated serum

In this study, a total of 15 metabolites in medicated serum were characterized and identified, and the metabolites of naringenin, protocatechuic acid and catechin were used as examples to illustrate the inference process.

Compound M4: In the positive ion mode, the quasimolecular ion peak m/z 287 [M+H] +, retention time 11.89 min, and the molecular formula of C16H1405 was obtained. The mass-to-charge ratio is 14 more than that of naringenin in negative ion mode (M+CH2). Based on the phase II metabolic pathway, it is speculated that it is the methylation of naringenin. The possible metabolic pathway is shown in **Figure 5A**.

Compound M5: In the positive ion mode, the quasimolecular ion peak m/z 331 [M+H] +, retention time 2.78 min, and the molecular formula of C13H14010 was obtained. The mass-to-charge ratio is 176 more than that of protocatechuic acid in negative ion mode (M+C6H806). Based on the phase II metabolic pathway, it is speculated that it is glucuronidation of protocatechuic acid.

Compound M6: In the positive ion mode, the quasimolecular ion peak m/z 345 [M+H] +, retention time 6.93 min, and the molecular formula of C14H16010 was obtained. The mass-to-charge ratio is 190 more than that of protocatechuic acid in negative ion mode (M+C7H1006). Based on the phase II metabolic pathway, it is speculated that it is glucuronated O-Methy of protocatechuic acid. The possible metabolic pathway is shown in **Figure 5B**.

Compound M11: In the negative ion mode, the quasimolecular ion peak m/z 331 [M+H] -, retention time 0.79 min, and the molecular formula of C17H1607 was obtained. The mass-to-

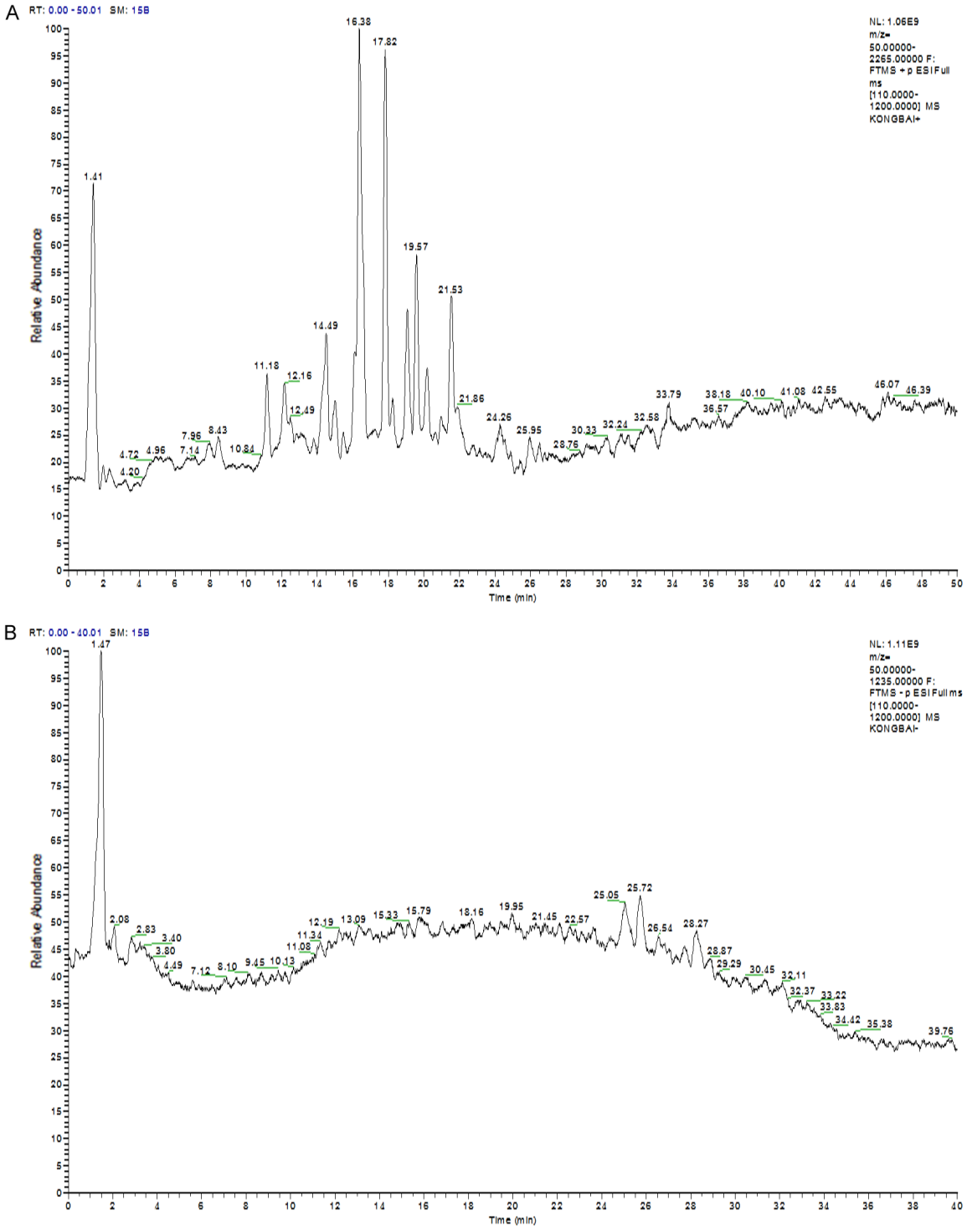

Figure 2. Total ion chromatograms of blank serum (a/b indicates positive/negative ions).

charge ratio is 42 more than that of catechin in positive ion mode (M+C2H2O). Based on the phase II metabolic pathway, it is speculated that it is the acetylation of catechin. The possible metabolic pathway is shown in **Figure 5C**.

Targets prediction

The SwissTargetPrediction and superpred databases retrieved 515 targets of Cynomorium ethyl acetate medicated serum components,

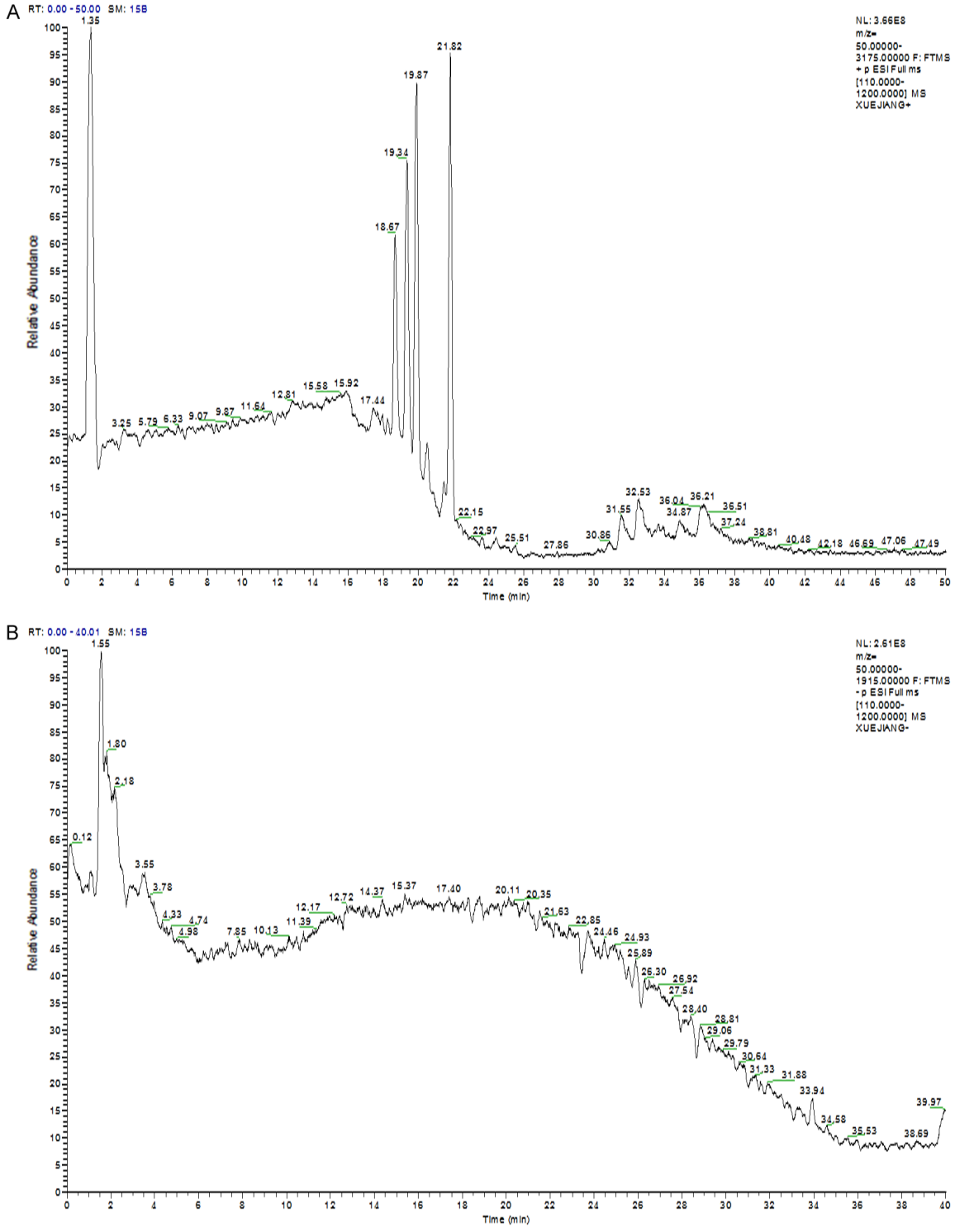

Figure 3. Total ion chromatograms of Cynomorium ethyl acetate medicated Serum (a/b indicates positive/negative ions).

and the TTD, OMIM, GeneCards and DrugBank databases retrieved 947 AD disease targets. Through the Venny diagram, we found that there were 143 common targets of Cynomorium ethyl acetate medicated serum components-AD disease, as shown in **Figure 6**.

Table 2. The mass spectrometry information of prototype components in Cynomorium ethyl acetate medicated serum

NO.	retention time/min	Ion mode	molecular weight		Mass error (ppm)	MS/MS Fragments	Compound	Molecular formula
			Theoretical value	measured value				
M1	33.95	[M+H] -	281.24751	281.24973	7.905	243.78976, 193.75041, 158.43777	oleic acid	C18H34O2
M2	33.47	[M+H] -	255.23186	255.23389	6.9536	219.84587, 158.33232, 117.05494	palmitic acid	C16H32O2
M3	25.94	[M+H] -	311.22169	311.22495	1.0475	213.03824, 145.05022, 112.98484	octadecenedioic acid	C18H32O4

Table 3. The mass spectrometry information of metabolites in Cynomorium ethyl acetate medicated serum

NO.	retention time/min	Ion mode	molecular weight		Mass error (ppm)	MS/MS Fragments	metabolic pathway	Compound	Molecular formula
			Theoretical value	measured value					
M4	11.89	[M+H] +	287.09140	287.09836	2.4243	205.05539, 163.94009, 84.96031	methylation	naringenin	C16H14O5
M5	2.78	[M+H] +	331.06597	331.06873	4.3367	221.03314, 203.02260, 84.96034	glucuronidation	protocatechuic acid	C13H14O10
M6	6.93	[M+H] +	345.08162	345.08572	5.18812	235.99744, 203.02251, 163.94017	glucuronidated O-methyl conjugates	protocatechuic acid	C14H16O10
M7	1.21	[M+H] +	183.06519	183.06255	-4.44211	141.11360, 125.02115, 113.96421	methylation	vanillic acid	C9H10O4
M8	2.59	[M+H] +	345.08162	345.08566	3.17074	235.99776, 163.94041, 135.94560	glucuronidation	vanillic acid	C14H16O10
M9	1.29	[M+H] -	185.04445	185.04298	-4.94404	158.44545, 117.05489, 87.04411	hydrolysis	vanillic acid	C8H10O5
M10	24.63	[M+H] -	315.25299	315.25623	-4.02775	243.03325, 219.01901, 201.00832	oxidation	oleic acid	C18H36O4
M11	0.79	[M+H] -	331.08123	331.08969	3.55526	257.08899, 185.03043, 157.03505	acetylation	catechin	C17H16O7
M12	2.27	[M+H] -	216.98014	216.98059	2.07392	172.99037, 160.84166, 1117.05497	sulfate esterification	salicylic acid	C7H6O6S
M13	2.78	[M+H] +	331.06597	331.06873	3.33671	260.03448, 208.00284, 84.96034	hydroxylation and glucuronidation	salicylic acid	C13H14O10
M14	22.15	[M+H] -	121.02841	121.02894	4.37914	100.92513, 87.04413, 71.04908	deoxidation	salicylic acid	C7H6O2
M15	3.04	[M+H] +	151.03897	151.03517	-2.51591	128.01967, 108.08124, 93.05779	methylation	p-hydroxybenzoic acid	C8H8O3
M16	2.98	[M+H] -	216.98014	216.98068	2.48871	172.99031, 142.97949, 129.0002	sulfate esterification	p-hydroxybenzoic acid	C7H6O6S
M17	2.78	[M+H] +	331.06597	331.06873	3.33671	221.03314, 203.02260, 84.96034	hydroxylation and glucuronidation	p-hydroxybenzoic acid	C13H14O10
M18	22.94	[M+H] -	121.02841	121.02874	2.72663	99.92513, 87.04412, 76.31445	deoxidation	p-hydroxybenzoic acid	C7H6O2

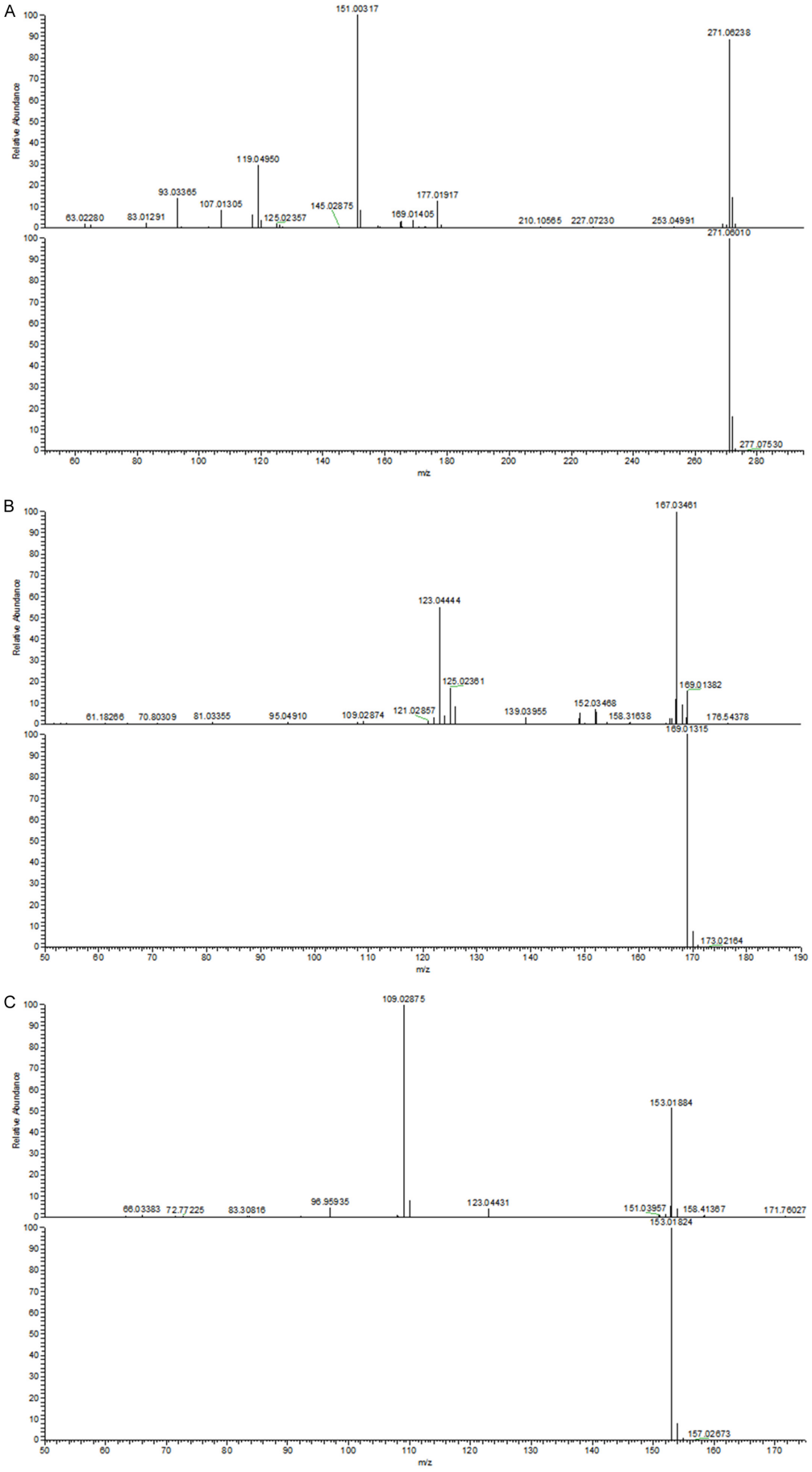
A
151.00317
271.06238
119.04950
93.03365
107.01305
145.02875
177.01917
63.02280
83.01291
125.02357
169.01405
210.10565
227.07230
253.04991
271.06010
277.07530
Relative Abundance
m/z
B
167.03461
123.04444
125.02361
169.01382
61.18266
70.80309
81.03355
95.04910
109.02874
121.02857
139.03955
152.03468
158.31638
176.54378
169.01315
173.02164
Relative Abundance
m/z
C
109.02875
153.01884
66.03383
72.77225
83.30816
96.95935
123.04431
151.03957
158.41367
171.76027
153.01824
157.02673
Relative Abundance
m/z

Figure 4. The secondary mass spectrum in negative ion mode. A: Naringenin; B: Gallic acid; C: Protocatechuic acid.

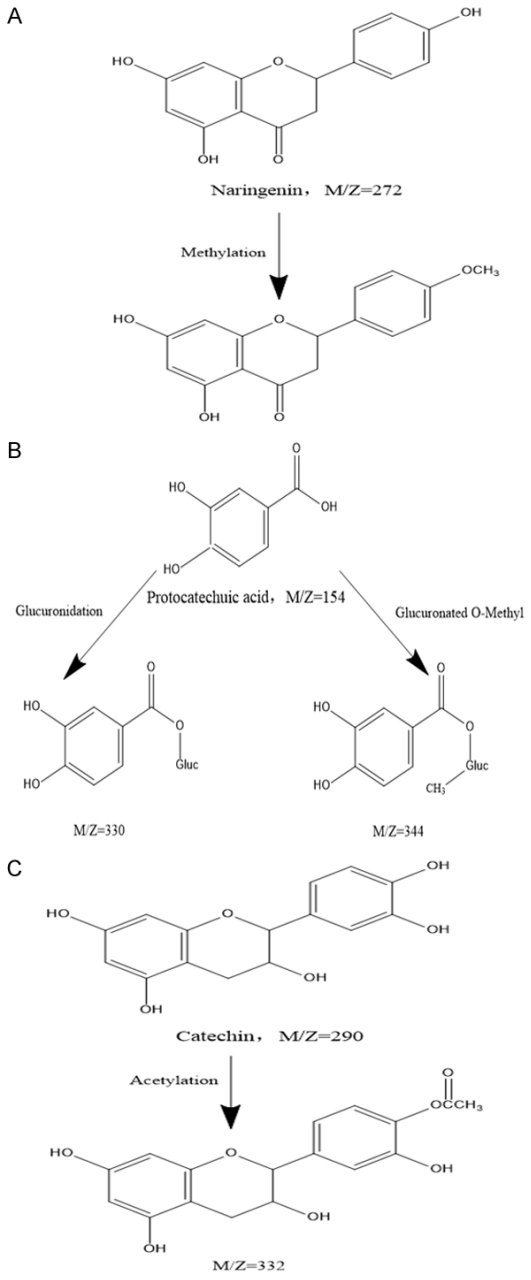

Figure 5. Metabolic pathway derivation diagram. A: Methylation of naringenin; B: Glucuronidation and glucuronated O-Methy of protocatechuic acid; C: Acetylation of catechin.

Construction the network of Cynomorium ethyl acetate medicated serum components-AD disease

In the network diagram of Cynomorium ethyl acetate medicated serum components-AD disease targets, the yellow nodes represent the Cynomorium ethyl acetate medicated serum components, the green nodes represent the gene targets, and the degree of a node represents the number of edges connected to the node in the network. According to the topological properties of the network, we selected targets with larger degree values for analysis, and the targets with more components connected may be the key targets for the effect of components. We performed a topological analysis of **Figure 7** to find the number of components acting on the targets, among them, M10: 9, 10-dihydroxystearic acid (degree = 57), M4: methylation of naringenin (degree = 55), M3: octadecenedioic acid (degree = 54), M1: oleic acid (degree = 51), M2: palmitic acid (degree = 45), M7: methylation of vanillic acid (degree = 37), M11: acetylation of catechins (degree = 35), M15: methylation of p-hydroxybenzoic acid (degree = 27), M18: deoxidation of p-hydroxybenzoic acid (degree = 25), M14: deoxidation of salicylic acid (degree = 25), these components may play an important role in the treatment of AD.

Screen key targets

We imported 143 common targets into STRING, the results are shown in **Figure 8** (the thickness of the lines in the figure represents the strength of the force), the results were exported in the form of text, and then imported them into Cytoscape software, the nodes with Degree and Closeness greater than the average value were selected as key targets. The average Degree of each node in the network is 5.625, the average Closeness of each node in the network is 0.378, and the average Betweenness of each node in the network is 0.028, among them, there are 13 targets whose Degree, Closeness and Betweenness all greater than the average value, including SRC, MAPK1, PIK3CA, PTPN11, FYN, VEGFA, MAPK8, MAPK14, NFKB1, ESR1, NR3C1, PRKCD, MAPT, we speculated that these 13 targets may be the key targets of Cynomorium ethyl acetate in the treatment of AD, the highest value is SRC, which can interact with 32 proteins, followed by MAPK1, PIK3CA and PTPN11, which can interact with 25, 22 and 21 proteins respectively.

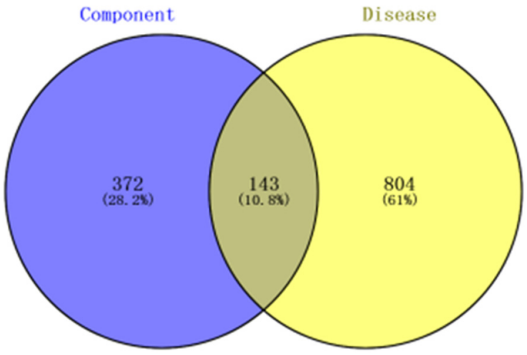

Figure 6. Venn diagram of common targets.

Results of GO and KEGG enrichment analysis

In the GO functional analysis, a total of 927 items were obtained, including 675 BP, 100 CC, and 152 MF. According to the size of the *P* value, the study used bar chart to list the top GO enrichment analysis results, and the top 10 results of each category are shown in **Figure 9A**.

The top 10 biology process listed include neuron death, regulation of neuron death, regulation of reactive oxygen species metabolic process, cognition, reactive oxygen species metabolic process, regulation of membrane potential, positive regulation of anion transport, response to amyloid-beta, positive regulation of reactive oxygen species metabolic process, and amyloid-beta metabolic process. The top 10 cellular components listed include membrane raft, membrane microdomain, synaptic membrane, postsynaptic membrane, neuronal cell body, integral component of presynaptic membrane, vesicle lumen, presynapse, intrinsic component of presynaptic membrane, and cytoplasmic vesicle lumen. The top 10 molecular function listed include postsynaptic neurotransmitter receptor activity, neurotransmitter receptor activity, protein tyrosine kinase activity, nuclear receptor activity, transcription factor activity, transmembrane receptor protein tyrosine kinase activity, neurotransmitter receptor activity involved in regulation of postsynaptic membrane potential, extracellular ligand-gated ion channel activity, and transmitter-gated ion channel activity.

In the KEGG enrichment analysis, a total of 96 major signaling pathways were obtained. According to the count value, the study used a bubble chart to list the top 30 entries, as shown in **Figure 9B**, including Alzheimer disease, pathways of neurodegeneration-multiple disease, neuroactive ligand-receptor interaction, calcium signaling pathway, proteoglycans in cancer, RAS signaling pathway, diabetic cardiomyopathy, MAKP signaling pathway, chemical carcinogenesis-receptor activation, lipid and atherosclerosis, herpesvirus infection, prostate cancer, central carbon metabolism in cancer, AGE-RAGE signaling pathway in diabetic complications, HIF-1 signaling pathway, relaxin signaling pathway, fluid shear stress and atherosclerosis, endocrine resistance, neurotrophin signaling pathway, EGFR tyrosine kinase inhibitor resistance, IL-17 signaling pathway, chagas disease, C-type lectin receptor signaling pathway, PD-L1 expression and PD-1 checkpoint pathway in cancer, prolactin signaling pathway, adherens junction, pancreatic cancer, cocaine addiction, nicotine addiction, and bladder cancer.

Analysis results of multidimensional network diagram

In order to further confirm the important role of key components in Cynomorium ethyl medicated serum in the treatment of AD, a component-target-pathway network diagram was constructed, including 167 nodes, the yellow nodes represent the components of Cynomorium ethyl acetate medicated serum, the purple nodes represent key targets and green nodes represent pathways. From the interaction relationship between each node of the multidimensional network diagram, the relationship between component-target-pathway can be obtained, as shown in **Figure 10**.

Discussion

With a non-vascular route of drug administration once a day for 1 week, the drug concentration in the blood reaches a steady-state blood drug concentration. At this time, the drug absorption rate and elimination rate reach a balance. Therefore, in this experiment the rats were given intragastric administration once a day, and blood was collected after continuous administration for 10 days.

There are many chemical components in traditional Chinese medicine, but the components absorbed into the blood have the best effect [8, 9]. Traditional Chinese medicines are mostly

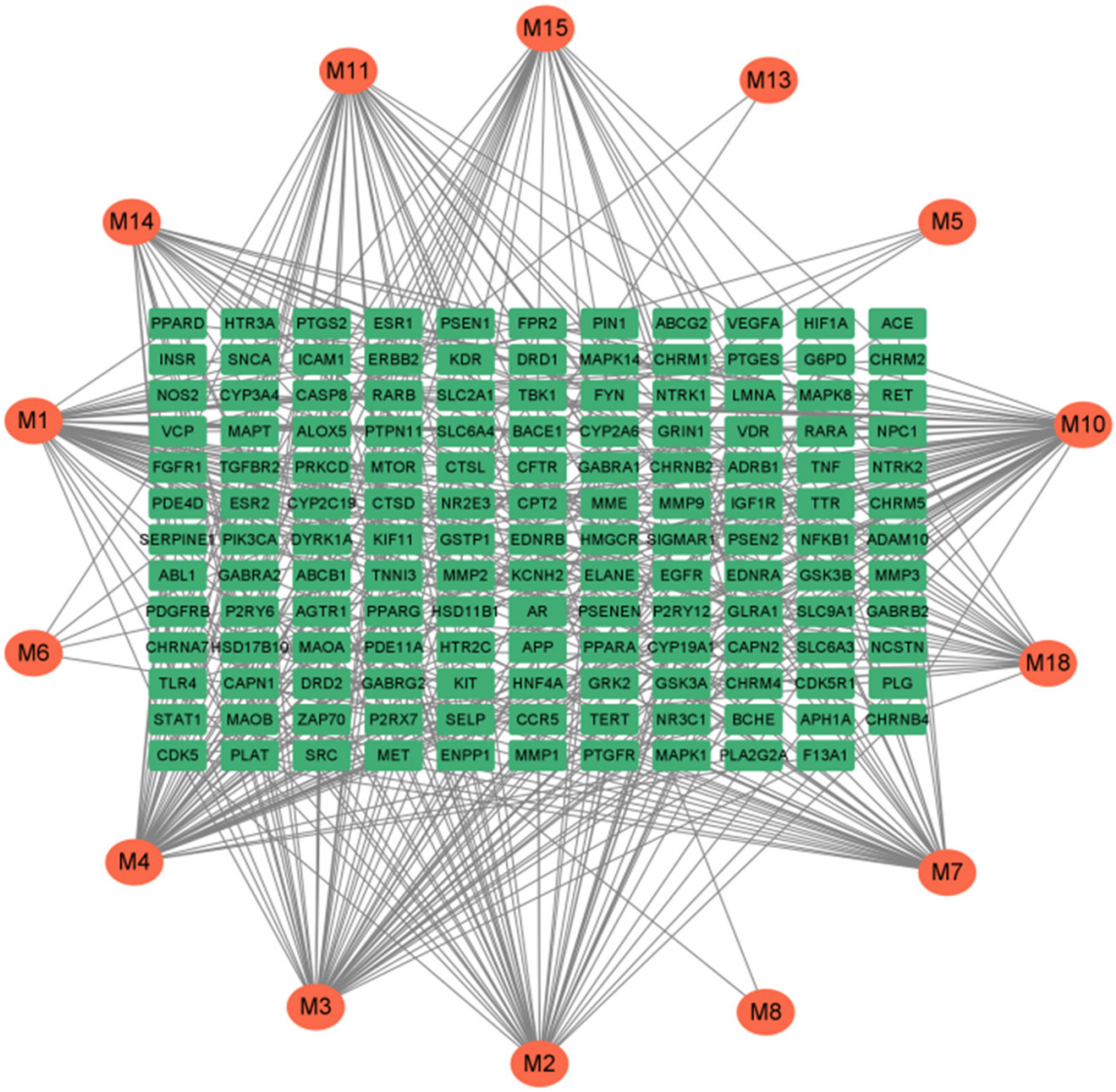

Figure 7. The network of Cynomorium ethyl acetate medicated serum components-AD disease.

administered orally. After oral administration, the drug components are directly absorbed into the blood through the digestive tract; or decomposed into secondary metabolites by the action of digestive juices, digestive enzymes and intestinal flora to be absorbed into the blood; or they are metabolized into active metabolites by liver microsomal enzymes. Regardless of the route, the effective substance must be transported to the target with blood as a medium to produce a drug effect. Therefore, the medicated serum is the "preparation" that really works, and the components contained in the serum are the direct-acting substances in the body of the traditional Chinese medicine.

The content of active ingredients in traditional Chinese medicine is low, so few active ingredients enter the body, and there are few metabolites [10]. The HPLC-Q-Exactive-MS/MS technology used in this experiment can not only provide accurate molecular weights of precursor ions and multi-level fragment ions, but also has fast scanning speed and high sensitivity. It is an ideal tool for the identification of components into the body. Combined with Xcalibur 3.0 software, it can assist in identifying the molecular weight and mass spectrometry fragment information of prototype components and metabolites in blood. The combination of the two kinds of software can analyze the

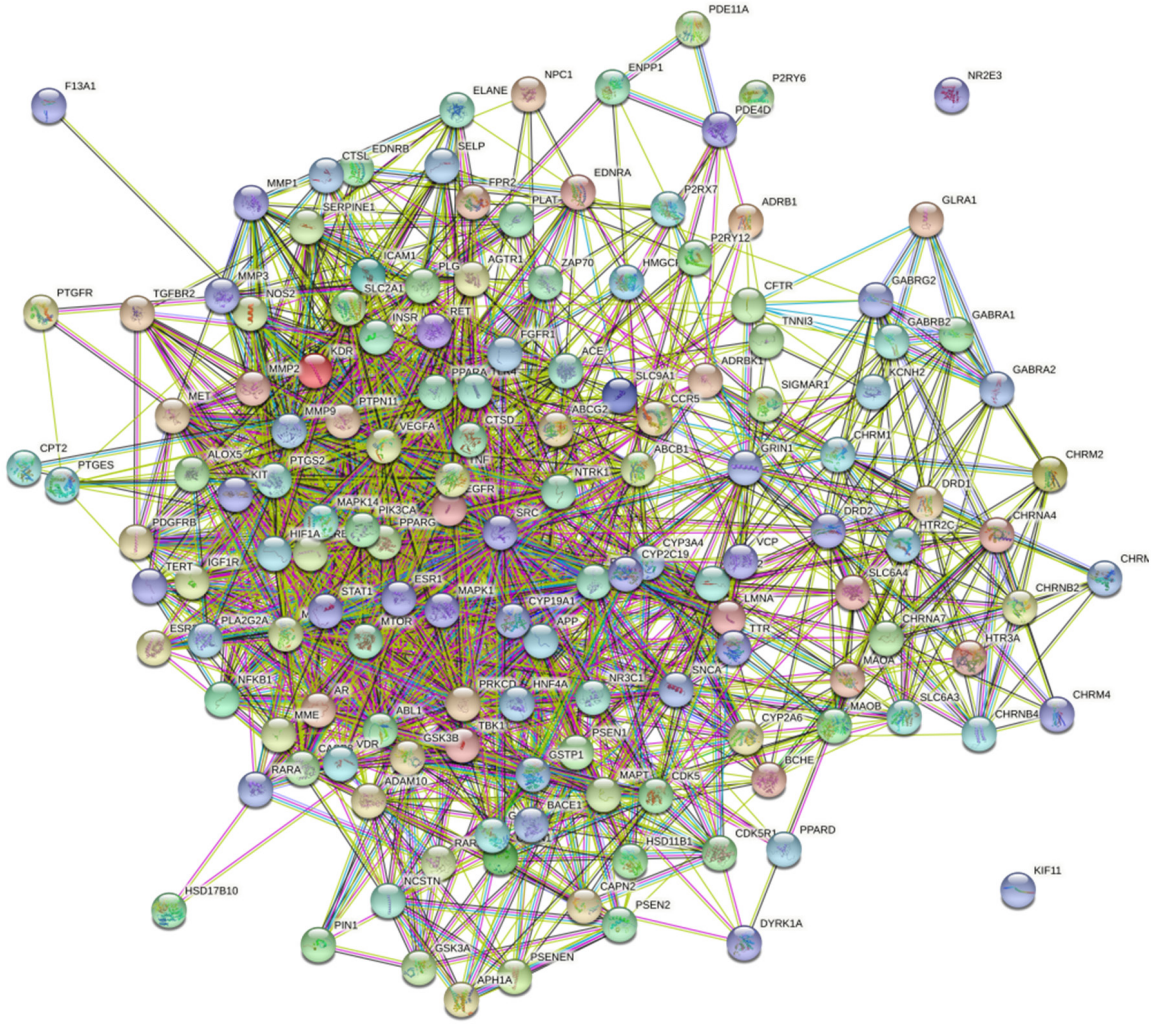

Figure 8. Protein-protein interaction network of the key targets.

components of the medicated serum more comprehensively.

The endogenous components of biological samples have a great influence on the detection of blood components, so pretreatment of biological samples is required to reduce the interference of endogenous components [11, 12]. The protein precipitation rate of acetonitrile is the highest among various precipitants, so in this experiment, we used the method of acetonitrile to deprecipitate the protein to pretreat the serum.

Through the analysis of the medicated serum components in this experiment, we found that there were 3 prototype components: oleic acid, palmitic acid, and octadecadienoic acid. There were 15 metabolites, of which 2 metabolites were derived from protocatechuic acid, 3 metabolites were derived from vanillic acid, 3 metabolites were derived from salicylic acid, 4 metabolites were derived from p-hydroxybenzoic acid, naringenin, oleic acid and catechin generated one metabolite respectively. According to the metabolic law, the phase I metabolism mainly occurs through hydrolysis, hydroxylation, and deoxygenation, and the phase II metabolism mainly occurs via methylation, acetylation, sulfate esterification, and glucuronidation. Some researchers have found that naringenin, as a flavonoid, can cross the blood-brain barrier, promote axonal regeneration, and improve cognition and learning ability, playing an important role in the treatment of neurodegenerative diseases such as AD [13, 14]. Oleic acid can improve cognitive and memory impairment, Oleic acid has been identified as an excellent

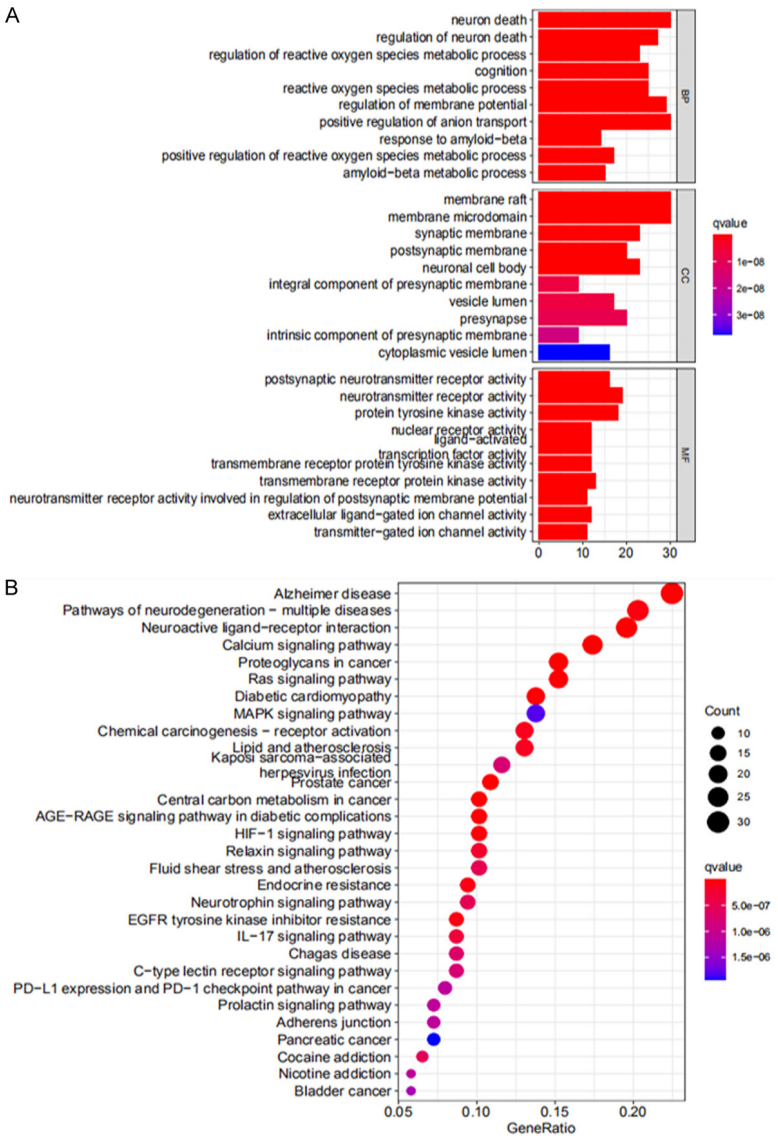

Figure 9. The results of GO functional analysis and KEGG enrichment analysis. A: Bar chart of the results of the GO functional analysis; B: Bubble chart of the results of the KEGG enrichment analysis.

inhibitors of Aβ40 or Aβ42 fibrillogenesis [15, 16]. Palmitic acid is a saturated fatty acid whose high consumption is largely associated with the development of different metabolic alterations and is considered a risk factor for AD, palmitic acid may serve as a biomarker for the treatment of AD [17, 18]. Vanillic acid has good blood-brain barrier penetration, it can stimulate mitochondrial biogenesis in neuronal cells, and change the expression of some genes related to neuronal differentiation, which can be used as a potential neuroprotective agent [19, 20]. As a flavonoid, catechin has the ability to cross the blood-brain barrier, it protects glial cells by reducing oxidative stress, it also attenuate glutamate-induced excitotoxicity and reduces neuroinflammation, it has properties of the treatment of pathological processes associated with aging and degeneration [21, 22].

Through the analysis of the targets, 13 core targets were obtained. The highest value was SRC, which could interact with 32 proteins, followed by MAPK1, PIK3CA and PTPN11, which could interact with 25, 22 and 21 proteins respectively. SRC is widely involved in physiological activities such as proliferation and division of neurons in brain tissue, it selectively block phosphorylation signaling of SRC kinases and reduces the delayed death of neurons [23, 24]. MAPK1 is a key kinase in the MAPK signaling pathway, as a protein-coding gene, MAPK1 is involved in various cellular processes such as proliferation, differentiation, transcriptional regulation, and plays an important role in the migration and growth of neural cells [25, 26]. In a physiological state, PIK3CA gene is expressed in brain, lung and other tissues, and regulates many important physiological functions such as cell proliferation, differentiation, survival, etc [27]. PTPN11 gene, also known as SHP2 gene, interacts with tau protein to generate Tau-SHP2 complex, the level of Tau-SHP2 complex in AD patients is increased, which plays an important role in the occurrence and development of AD disease [28].

Through the analysis of the KEGG pathway, a total of 96 pathways were obtained, among which calcium signaling pathway, ras signaling pathway, and MAPK signaling pathway were highly enriched. Calcium signaling pathway is regulated by presenilin, genetic mutation of

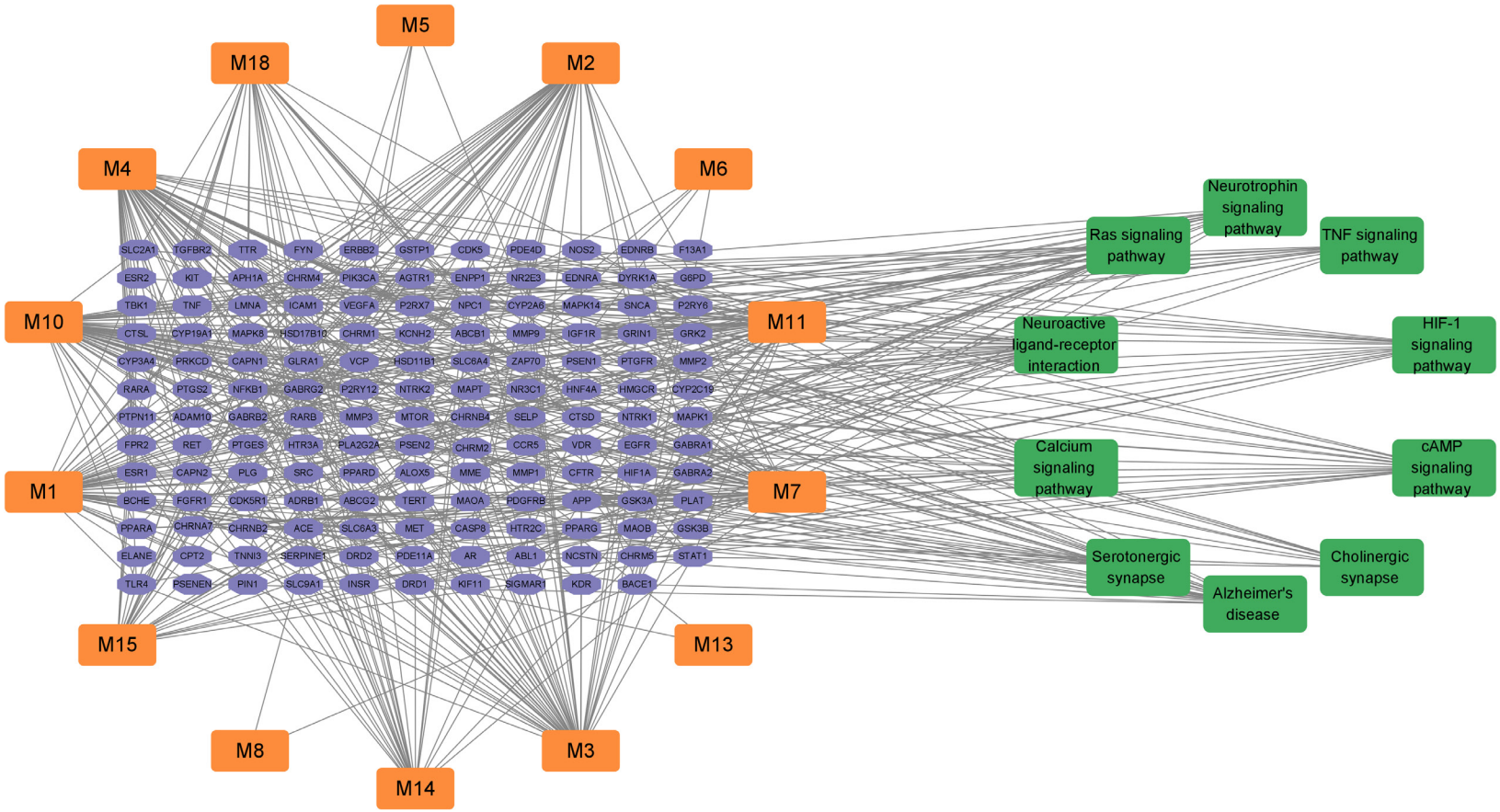

Figure 10. The network of component-target-pathway.

presenilin in neurons can impair calcium regulation and reduce its ability to deal with oxidative stress, which leads to cell death and promotes AD [29, 30]. RAS is an important part of nerve plaques. Some studies have found that by blocking the energy metabolism and oxidative stress of RAS in the brain of AD mice, it can reduce the inflammatory response and the deposition of beta amyloid, improve the memory and delay the AD disease progression [31-33]. Inhibition of MAPK signaling can reduce the release of neuroinflammatory factors, protect dopaminergic neurons and improve behavioral disorders [34].

Acknowledgements

We thank Professor QuBi from the School of Pharmacy, Inner Mongolia Medical University for the identification of Cynomorium. This research was supported by the Natural Science Foundation of Inner Mongolia Autonomous Region (NO. 2020MS08038).

Disclosure of conflict of interest

None.

Address correspondence to: Ruilan Han, School of Pharmacy, Inner Mongolia Medical University, Hohhot 010110, Inner Mongolia Autonomous Region, China. Tel: +86-0471-6653132; E-mail: 980144634@qq.com

References

[1] Cabrera-Pardo J, Fuentealba J, Gavilán J, Cajas D, Becerra J and Napiórkowska M. Exploring the multi-target neuroprotective chemical space of Benzofuran scaffolds: a new strategy in drug development for Alzheimer's disease. Front Pharmacol 2020; 10: 1679.

[2] Meng HC, Wang S, Li Y, Kuang YY and Ma CM. Chemical constituents and pharmacologic actions of Cynomorium plants. Chin J Nat Med 2013; 11: 321-329.

[3] Lu Y, Wang Q, Melzig M and Jenett-Siems K. Extracts of Cynomorium songaricum protect human neuroblastoma cells from beta-amyloid25-35 and superoxide anion induced injury. Pharmazie 2009; 64: 609-612.

[4] Tian FZ, Chang HS, Liu JX, Zheng J, Cheng D and Lu Y. Cynomorium songaricum extract alleviates memory impairment through increasing CREB/BDNF via suppression of p38MAPK/ERK pathway in ovariectomized rats. Evid Based Complement Alternat Med 2019; 2019: 9689325.

[5] Liang Y, Li L, Cai Y, Xu LB, Xie FF, Liang DL and Chen FL. Analysis of chemical constituents in ethyl acetate extract of Taxilli Herba by UPLC-Q-Exactive-MS and screening of potential xanthine oxidase inhibitors. Zhongguo Zhong Yao Za Zhi 2022; 47: 972-979.

[6] Chen J, Chen Y, Du X, Tao H, Pu Z, Shi X, Yue S, Zhou G, Shang E, Tang Y and Duan J. Fuzzy identification of bioactive components for different efficacies of rhubarb by the back propagation neural network association analysis of UPLC-Q-TOF/MS E and integrated effects. Chin Med 2022; 17: 50.

[7] Chen Y, Cai X, Li G, He X, Yu X, Yu X, Xiao Q, Xiang Z and Wang C. Chemical constituents of radix Actinidia chinensis planch by UPLC-QTOF-MS. Biomed Chromatogr 2021; 35: e5103.

[8] Ma FX, Xue PF, Wang YY, Wang YN and Xue SY. Research progress of serum pharmacochemistry of traditional Chinese medicine. Zhongguo Zhong Yao Za Zhi 2017; 42: 1265-1270.

[9] Wu R, Liang Y, Xu M, Fu K, Zhang Y, Wu L and Wang Z. Advances in chemical constituents, clinical applications, pharmacology, pharmacokinetics and toxicology of erigeron breviscapus. Front Pharmacol 2021; 12: 656335.

[10] Guo Y, Lü S, Yang B, Li G, Ma W, Guo Q, Wang Q and Kuang H. HPLC-MS/MS method for the determination and pharmacokinetic study of six compounds against rheumatoid arthritis in rat plasma after oral administration of the extract of Caulophyllum robustum Maxim. J Pharm Biomed Anal 2020; 181: 112923.

[11] Sweeney C, Park Y and Kim J. Comparison of sample preparation approaches and validation of an extraction method for nitrosatable pesticides and metabolites in human serum and urine analyzed by liquid chromatography-Orbital ion trap mass spectrometry. J Chromatogr A 2019; 1603: 83-91.

[12] Haginaka J. Development of HPLC packing materials for drug analysis and their applications. Yakugaku Zasshi 1996; 116: 473-490.

[13] Youdim KA, Qaiser MZ, Begley DJ, Rice-Evans CA and Abbott NJ. Flavonoid permeability across an in situ model of the blood-brain barrier. Free Radic Biol Med 2004; 36: 592-604.

[14] Lawal M, Olotu F and Soliman M. Across the blood-brain barrier: neurotherapeutic screening and characterization of naringenin as a novel CRMP-2 inhibitor in the treatment of Alzheimer's disease using bioinformatics and computational tools. Comput Biol Med 2018; 98: 168-177.

[15] El Shatshat A, Pham AT and Rao PPN. Interactions of polyunsaturated fatty acids with amyloid peptides Aβ40 and Aβ42. Arch Biochem Biophys 2019, 663: 34-43.

[16] Sirichaiwetchakoon K, Suksuphew S, Srisawat R and Eumkeb G. Butea superba Roxb. Ex-

tract ameliorates scopolamine-induced cognitive and memory impairment in aged male rats. Evid Based Complement Alternat Med 2021; 2021: 2703138.
[17] Meng S, Li S, Chen H, Deng C, Meng Z and Wang Y. Therapeutic effects and metabolic spectrum of traditional Chinese medicine Hengqing II prescription on Alzheimer's disease. Evid Based Complement Alternat Med 2022; 2022: 5912396.
[18] Sánchez-Alegría K, Bastián-Eugenio C, Vaca L and Arias C. Palmitic acid induces insulin resistance by a mechanism associated with energy metabolism and calcium entry in neuronal cells. FASEB J 2021; 35: e21712.
[19] Ay M. Vanillic acid induces mitochondrial biogenesis in SH-SY5Y cells. Mol Biol Rep 2022; 49: 4443-4449.
[20] Siraj M, Howlader M, Rahaman M, Shilpi J and Seidel V. Antinociceptive and sedative activity of vernonia patula and predictive interactions of its phenolic compounds with the cannabinoid type 1 receptor. Phytother Res 2021; 35: 1069-1079.
[21] Vidak M, Rozman D and Komel R. Effects of flavonoids from food and dietary supplements on glial and glioblastoma multiforme cells. Molecules 2015; 20: 19406-19432.
[22] Kubicova L, Bachmann G, Weckwerth W and Chobot V. (±)-Catechin-A mass-spectrometry-based exploration coordination complex formation with Fe II and Fe III. Cells 2022; 11: 958.
[23] Moysenovich A, Tatarskiy V, Yastrebova M, Bessonov I, Arkhipova A, Kolosov A, Davydova L, Khamidullina A, Bogush V, Debabov V, Shaitan K, Shtil A and Moisenovich M. Akt and Src mediate the photocrosslinked fibroin-induced neural differentiation. Neuroreport 2020; 31: 770-775.
[24] Mao X, Pan C, Huang P, Liu Y, Wang C, Yan L, Hu B, Chang X, He K, Mu H, Li Q, Sun K, Fan J and Han J. Levo-tetrahydropalmatine attenuates mouse blood-brain barrier injury induced by focal cerebral ischemia and reperfusion: involvement of Src kinase. Sci Rep 2015; 5: 11155.
[25] Bankston A, Li W, Zhang H, Ku L, Liu G, Papa F, Zhao L, Bibb J, Cambi F, Tiwari-Woodruff S and Feng Y. P39, the primary activator for cyclin-dependent kinase 5 (Cdk5) in oligodendroglia, is essential for oligodendroglia differentiation and myelin repair. J Biol Chem 2013; 288: 18047-18057.
[26] Luo F, Shi J, Shi Q, Xu X, Xia Y and He X. Mitogen-activated protein kinases and hypoxic/ischemic nephropathy. Cell Physiol Biochem 2016; 39: 1051-1067.
[27] Broderick D, Di C, Parrett T, Samuels Y, Cummins J, McLendon R, Fults D, Velculescu V, Bigner D and Yan H. Mutations of PIK3CA in anaplastic oligodendrogliomas, high-grade astrocytomas, and medulloblastomas. Cancer Res 2004; 64: 5048-5050.
[28] Kim Y, Liu G, Leugers C, Mueller J, Francis M, Hefti M, Schneider J and Lee G. Tau interacts with SHP2 in neuronal systems and in Alzheimer's disease brains. J Cell Sci 2019; 132: jcs229054.
[29] Chernyuk D, Zernov N, Kabirova M, Bezprozvanny I and Popugaeva E. Antagonist of neuronal store-operated calcium entry exerts beneficial effects in neurons expressing PSEN1ΔE9 mutant linked to familial Alzheimer disease. Neuroscience 2019; 410: 118-127.
[30] Galla L, Redolfi N, Pozzan T, Pizzo P and Greotti E. Intracellular calcium dysregulation by the Alzheimer's disease-linked protein presenilin 2. Int J Mol Sci 2020; 21: 770.
[31] Li K, Li J, Zheng J and Qin S. Reactive astrocytes in neurodegenerative diseases. Aging Dis 2019; 10: 664-675.
[32] Farina C, Aloisi F and Meinl E. Astrocytes are active players in cerebral innate immunity. Trends Immunol 2007; 28: 138-145.
[33] Assefa B, Gebre A and Altaye B. Reactive astrocytes as drug target in Alzheimer's disease. Biomed Res Int 2018; 2018: 4160247.
[34] Yao C, Liu X, Zhou Z, Xiang Y, Yuan S, Xie W, Zhou M, Hu Z, Li Y, Ji A and Cai T. Melatonin attenuates expression of cyclooxygenase-2 (COX-2) in activated microglia induced by lipopolysaccharide (LPS). J Toxicol Environ Health A 2019; 82: 437-446.